AUDITORY NERVE TERMINALS AND COCHLEAR NUCLEUS NEURONS:

ENDBULBS OF HELD AND SPHERICAL BUSHY CELLS

David K. Ryugo and Seishiro Sento

OUTLINE

Advances in Speech, Hearing and Language Processing
Volume 3, Part A, pages 19-40

ISBN: 1-55938-430-1

ABSTRACT

The central axons of type I spiral ganglion neurons in cats were stained with horseradish peroxidase (HRP) using both intracellular and extracellular labeling methods. Forty-six fibers were electrophysiologically characterized by recording with micropipettes inserted into the axon and then labeled by intracellular injections of HRP through the same pipettes. This method allowed us to describe structure-function relationships in the anteroventral cochlear nucleus for the prominent axosomatic endings of auditory nerve fibers called endbulbs of Held. The largest endbulbs arise from fibers having a characteristic frequency (CF, that tonal frequency to which a fiber is most sensitive) between 1-4 kHz; smaller endbulbs can arise from fibers of any CF. Endbulb size is not correlated to fiber spontaneous discharge rate (SR). Dividing the endbulb's silhouette area by the silhouette perimeter, however, produced a ratio that reliably indicated SR fiber grouping for individual endbulbs. Extracellularly labeled pairs of auditory nerve fibers were studied which gave rise to endbulbs that converged onto the same cell body. Pairs of endbulbs have similar form factor values despite the wide range of values for the endbulb population. These data imply that endbulbs converging upon the cell body of a spherical bushy cell arise from fibers of the same SR group.

1. INTRODUCTION

In the auditory nerve of mammals, 95 percent of the fibers are myelinated and conduct acoustic information from inner hair cell receptors (Spoendlin, 1973; Arnesen and Osen, 1978; Liberman and Oliver, 1984). This fiber system originates from type I spiral ganglion neurons and is presumably for the rapid transmission of activity arising from a punctate region of the basilar membrane. Type I neurons, however, are not a homogeneous population because they can differ across a variety of morphological and physiological characteristics (Kiang et al., 1965; Liberman, 1978, 1982; Evans and Palmer, 1980; Fekete et al., 1984; Rouiller et al., 1986; Ryugo and Rouiller, 1988).

Spontaneous activity is one important property of these myelinated axons. All-or-none discharges can range from near zero to greater than 100 spikes per second (s/s), and occur in the absence of experimenter-controlled acoustic stimulation (Walsh et al., 1972; Evans, 1975). The spontaneous discharge rate (SR) of a fiber is indicative of its sensitivity to sound and its maximum discharge rate (Kiang et al., 1965; Liberman, 1978; Sachs and Abbas, 1974), and is correlated to distinctive features of the fiber's peripheral morphology (Liberman, 1982). High SR fibers ($>$ 18 s/s) have low thresholds to sounds and thick peripheral processes; in contrast, low SR fibers ($\leq$ 18 s/s) have high thresholds and exhibit thin peripheral processes. Because both SR groups can be found at all frequency values, they may subserve fundamentally different roles in hearing.

In the cochlear nucleus, the obligatory synaptic interruption of auditory nerve fibers provides the first site for recoding neural information arising in the cochlea. The auditory code (that is, the temporal pattern of spike discharges) entering the nucleus is qualitatively similar across all fibers for a broad range of stimulus conditions. In the cochlear nucleus, however, this code can be preserved or transformed (Pfeiffer, 1966). The separate kinds of output activity are sent to higher auditory centers and are thought to convey separate features of the acoustic information (Warr, 1982; Cant and Morest, 1984). The focus of this report is on the pathway which tightly couples neural activity to acoustic events and is hypothesized to maintain timing information.

In the anteroventral cochlear nucleus (AVCN), large endings of type I auditory nerve fibers, called endbulbs of Held, make axosomatic synapses with spherical bushy cells (Lenn and Reese, 1966; Ibata and Pappas, 1976; Cant and Morest, 1979; Ryugo and Fekete, 1982). Because of the regional overlap between endbulbs, anatomically-defined spherical bushy cells, and physiologically-defined primary-like units with prepotentials, it has been suggested that endbulbs ensure the 1-to-1 transfer of discharges in the auditory nerve fiber to the spherical bushy cell, producing the primarylike patterns observed in the nucleus (Pfeiffer, 1966; Bourk, 1976; Tsuchitani, 1978; Cant and Morest, 1984). If spherical bushy cells act as simple relays, then the population of primary-like units with prepotentials should reflect the physiological features of the population of auditory nerve fibers by which they are innervated. In the auditory nerve, approximately 30-40 percent of the fibers have spontaneous discharge rates (SR) below 18 s/s (Kiang et al., 1965; Liberman, 1978); in the AVCN however, the proportion of such primary-like units with prepotentials is 5-15% (Molnar and Pfeiffer, 1968; Bourk, 1976; T. Yin, personal communication). Because spontaneous activity in the ventral cochlear nucleus is derived from the auditory nerve (Koerber et al., 1966), the question arises as to how the primary activity from endbulbs is transferred to spherical bushy cells to produce the observed alteration of SR distribution in the nucleus.

In the present study, we used light and electron microscopic examination of endbulbs labeled with horseradish peroxidase to explore various structural mechanisms that might help explain the electrophysiological data. Because single auditory nerve fibers are intracellularly labeled after recording their physiological characteristics through the same micropipette, we can make direct correlations between a fiber's response properties and the morphological features of the endbulb and its postsynaptic neuron. We present light microscopic evidence suggesting that endbulbs of the same SR group converge together onto the cell body of the same spherical bushy cell, and that endbulbs of different SR groups do not.

2. MATERIALS AND METHODS

2.1 Animals and Surgical Preparation

A total of 37 cats, each weighing between 1.4 and 3.7 kg and in good health, were used in this study. Animals were anesthetized with intraperitoneal injections (0.2 ml per kg body weight) of diallyl barbituric acid (100 mg/ml) in urethane solution (400 mg/ml). Supplemental doses were periodically administered in order to maintain areflexia to paw pinches. The bulla and its bony septum were opened to allow for round window recordings and the external meati were cut just peripheral to the tympanic ring to allow insertion of the acoustic system. The skin and muscle layers of the head were removed so that the skull overlying the posterior fossa could be opened with rongeurs. The dura was reflected over the cerebellum, and the cerebellum was retracted revealing the auditory nerve between the internal auditory meatus and the cochlear nucleus. Micropipette electrodes were then placed into the nerve under direct visual control. Thirty-one cats were used to obtain intracellular data and 6 were used for extracellular data.

2.2 Intracellular Labeling

For each unit, a threshold tuning curve and a 15 or 30 second sample of spontaneous activity were obtained before and after the injection of HRP. The tip of the tuning curve was used to determine fiber characteristic frequency (CF), and spontaneous discharge rate (SR) was defined as spike activity (spikes per second, s/s) in the absence of sound controlled by the experimenter. Individual fibers were labeled by iontophoresing a 10 percent solution of HRP (Sigma, type VI) in 0.05 M Tris buffer (pH 7.3) containing 0.15 M KCl through micropipettes bevelled to a final impedence of 40-60 megohms.

2.3 Extracellular Injections

For 6 cats, extracellular injections were made using a glass micropipette filled with a solution of HRP (Sigma type VI, 20-30% w/v in 0.1 M Tris buffer, pH 7.6) inserted into the nerve under direct visual control; HRP was ejected electrophoretically (2 microamps, positive current, 50% duty cycle, 5 minutes) through the pipette tip (20-50 μm, I.D.).

2.4 Histology

Approximately 24 hours after the HRP injections, the cat was given a lethal dose of barbiturate, artificially respirated, and perfused intracardially with buffered fixatives. The perfusion solutions consisted of 50 ml of isotonic saline (37°C) with 0.1 percent $NaNO_2$ followed immediately by 500 ml of fixative (37°C) containing 0.5 percent paraformaldehyde, 1.0 percent glutaraldehyde, and 0.008 percent $CaCl_2$ in 0.12 M phosphate buffer (pH 7.4), and then 1500 ml of a second fixative (37°C) containing 1.25 percent paraformaldehyde, 2.5 percent glutaraldehyde, and 0.008 percent $CaCl_2$ in the same buffer solution. Following perfusion and decapitation, the head was immersed in the second fixative (5°C) with enough bone and tissue removed to expose the auditory nerve and cochlear nucleus to the fixative. After 12-24 hours, the brain was removed from the skull and the nerve and nucleus isolated in a single tissue block. Each block was embedded in gelatin-albumin, sectioned at 40-60 μm thickness using a Vibratome, and kept in serial order. The sections were rinsed several times in 0.1 M Tris buffer (pH 7.6) and then incubated for one hour in a solution of 0.5 percent $CoCl_2$ in Tris buffer. These sections were washed in Tris buffer, washed in 0.1 M phosphate buffer (pH 7.3), incubated for one hour in a solution of 0.05 percent 3,3'-diaminobenzidine (DAB) and 1 percent dimethylsulfoxide in phosphate buffer (pH 7.3), and then incubated another hour in the DAB solution containing 0.01 percent H_2O_2. Sections were washed and then mounted on glass microscope slides and counterstained with cresyl violet, or postfixed with 0.1 percent OsO_4 for 15 minutes, stained *en bloc* with 1 percent uranyl acetate (overnight), dehydrated, infiltrated with Epon and then flat embedded in a drop of Epon between 2 sheets (each 2.5 x 7.5 cm) of Aclar (Ted Pella Inc.).

2.5. Reconstructions and Data Analysis

Only fibers that were well-characterized electrophysiologically and recovered with high confidence were used in this analysis. The presence of continuously negative DC potentials plus similarities between pre- and post-injection responses provided the evidence that the electrode tip remained inside the same fiber throughout the recording and injection period. When more than 1 fiber was injected in an auditory nerve, they were physiologically separated in CF and spatially separated according to the anterior, middle, or posterior third of the nerve. The position of the fiber's trajectory within the nerve matched the calculated position of the pipette tip at the time of injection and fiber CF was highly correlated with fiber trajectory within the cochlear nucleus for the present sample of recovered fibers.

Recovered HRP-labeled fibers appeared dark brown or black against the pale-staining tissue of the cochlear nucleus; furthermore, they exhibited distinct swellings at the tips of every terminal branch in the anteroventral cochlear nucleus, thereby providing light microscopic evidence that the ascending branch was completely stained. At the rostral terminus of the ascending branch

is typically found a large, axosomatic ending called the endbulb of Held (Ramon and Cajal, 1909; Ryugo and Fekete, 1982; Fekete et al., 1984). Our analysis focused on this large ending and its somatic contact.

"Coded" endbulbs and their postsynaptic spherical cell were drawn with the aid of a light microscope and drawing tube at a total magnification of x2000. Because endbulbs are a complex, three-dimensional structure, their parts often overlapped when they were reduced to a planar silhouette. In such instances, the overlapping parts were optically separated using different focal planes and drawn. The drawings of each endbulb were photographically enlarged to a final magnification of 3000x or 3750x; silhouette areas and perimeters were determined by computerized planimetry (Sigmascan, Jandel Scientific) for terminal endbulbs. The proportion, area divided by perimeter, produced a "form factor" (the μm unit was dropped) that we used to represent geometric complexity. The cell bodies of the postsynaptic spherical busy cells were similarly measured through the plane of the nucleolus. Drawings were "decoded" when all measurements were completed.

Endbulb measurements were analyzed with respect to fiber CF and SR. Fibers were assigned to the low SR group (SR $\leq$ 18 s/s) or the high SR group (SR $>$ 18 s/s). Our low SR group represents the combining of Liberman's (1978) low and medium SR groups; we combined the 2 groups because we could find no reliable morphological distinctions between them (Fekete et al., 1984; Rouiller et al., 1986; Ryugo and Rouiller, 1988; Sento and Ryugo, 1989; Ryugo and Sento, 1991). The cytoarchitectonic regions of the cochlear nucleus are used as previously defined (see Fig. 2, Fekete et al., 1984). Means, standard errors of the mean, Smirnov's p values (non-parametric, two-tailed), and correlation coefficients (r) with p values are provided when appropriate.

3. RESULTS

The light microscopic, intracellular data are based on 46 physiologically characterized auditory nerve fibers in 37 cochlear nuclei. Seven fibers were low SR, 9 were medium SR, and 30 were high SR; the CF range for all fibers was 0.2-28.2 kHz. The endbulb from 1 high SR fiber was subject to electron microscopic analysis. Each fiber gave rise to a single terminal endbulb of Held, which was operationally defined as a large, axosomatic termination at the tip of the ascending branch, composed of 14 or more components (lobules and swellings; see also Rouiller et al., 1986). As defined, terminal endbulbs were easily recognizable and distributed within the anterior division of the AVCN. An additional 19 pairs of converging endbulbs were labeled by extracellular injections of HRP and studied with the light microscope.

Figure 1. Photomicrograph of endbulbs from auditory nerve fibers of the different SR groups. The endbulb on the left is from a high SR fiber (CF = 1.1 kHz, SR = 56 s/s); that on the right is from a low SR fiber (CF = 1.0 kHz, SR = 0.01 s/s). These endbulbs are from the same cat but in opposite cochlear nuclei. Note that the endbulb from the low SR fiber has more and smaller lobulations than does the endbulb from the high SR fiber. Scale bar = 10 μm. (From Ryugo and Sento, 1991).

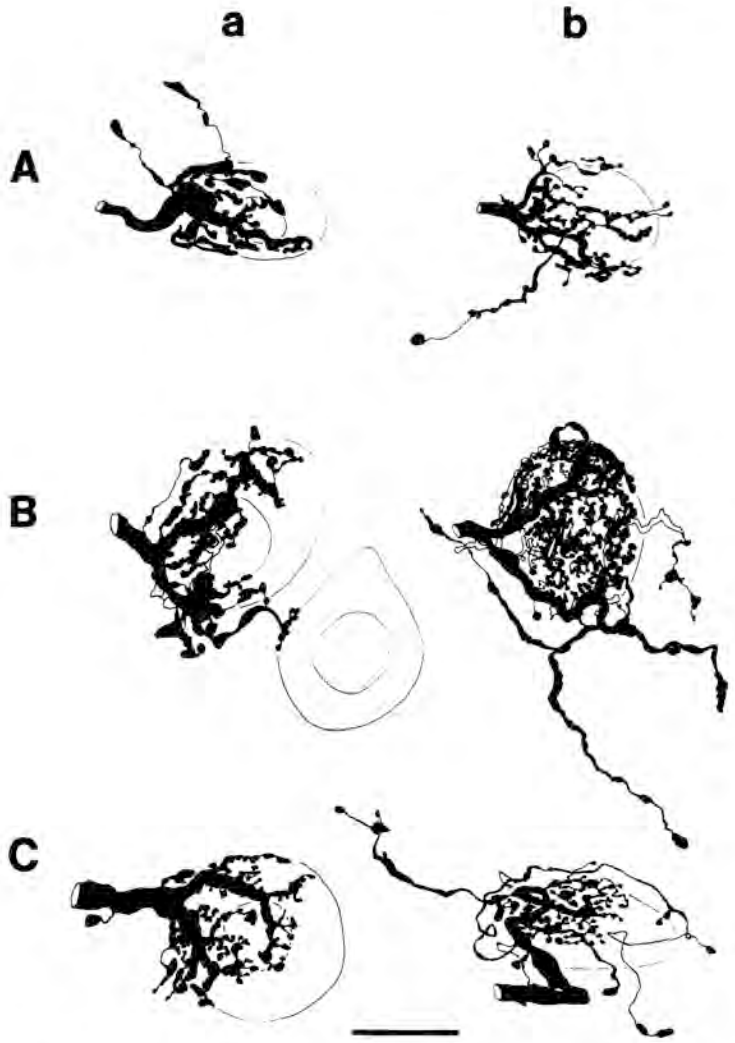

Figure 2. Drawing tube reconstructions of three pairs of endbulbs of Held (A-C). Each pair is from opposite cochlear nuclei of the same cat, representing roughly similar CF ranges but different SR groups. Endbulbs in column a are from high SR fibers and those in column b are from low SR fibers. See Table 1 for quantitative data on these endbulbs. Scale bar = 20 μm. (From Sento and Ryugo, 1989).

3.1 Endbulbs of Held: Intracellular Labeling

Endbulbs exhibit a wide variety in size and shape. In order to reduce inter-animal variation, pairs of fibers were selected such that members of each pair were of similar CF but different SR. Each fiber of a pair was injected in separate nerves, and one cat typically yielded 1-3 pairs. An example of an endbulb pair stained by this method is illustrated in Figure 1. Each endbulb consists of a highly branched, cup-shaped arborization that partially encloses the soma of a spherical bushy cell. The parent trunk divides into several thick, knobby branches that in turn generate a number of successively finer branches. The branches of the arborization display irregular varicosities and lobes, many of which are linked together by thin filamentous processes. Moreover, the appearance of endbulbs from the separate SR groupings is distinctive. The endbulb of the high SR fiber exhibits fewer but larger varicosities and associated terminal swellings. In contrast, the endbulb of the low SR fiber displays a delicate network of many small varicosities and associated terminal swellings.

Additional examples of endbulbs from physiologically characterized fibers are shown in Figure 2. Most elements of the endbulb appear in close apposition to the surface of the postsynaptic cell body and form part of the axosomatic contact. In addition, collateral processes of various lengths and branching patterns are frequently present which distribute *en passant* and terminal swellings away from the cell body but still to nearby regions (usually within 100 μm). When the swellings are found in neuropil, it is not possible to determine whether they contact distal parts of the same cell (Fig. 2Aa, 2Ab, 2Bb, 2Cb), although it is often clear that they contact a different cell (Fig. 2Ba). The presence or absence, length, or branching patterns of these collaterals does not appear to be related to the fiber's physiological response properties.

Endbulb Size

The silhouette area of individual endbulbs was used to represent size. Fiber CF is related to endbulb size (Fig. 3A). As fiber CF increases from 0.2 to approximately 4 kHz, so does the area of the endbulb ($n = 34$, correlation coefficient $= 0.48, p < 0.01$). As CF continues to increase above 4 kHz, endbulb area decreases ($n = 12$, correlation coefficient $= 0.66$, $p < 0.02$). The result is that the largest endbulbs originate from fibers having CFs between 1-4 kHz.

The area of the endbulb does not appear to be dramatically related to fiber SR (Fig. 3B). On average (mean $\pm$ s.e.m.), there are not statistically significant size differences for endbulbs of the two SR groups; endbulb area for high SR fibers equalled 271.6 ± 20.1 μm^2, whereas endbulb area for low-medium SR fibers equalled 230.5 ± 25.1 μm^2 ($p < 0.10$). These data are not affected by the size variations due to fiber CF (Fig. 3A): For a given CF range, endbulbs

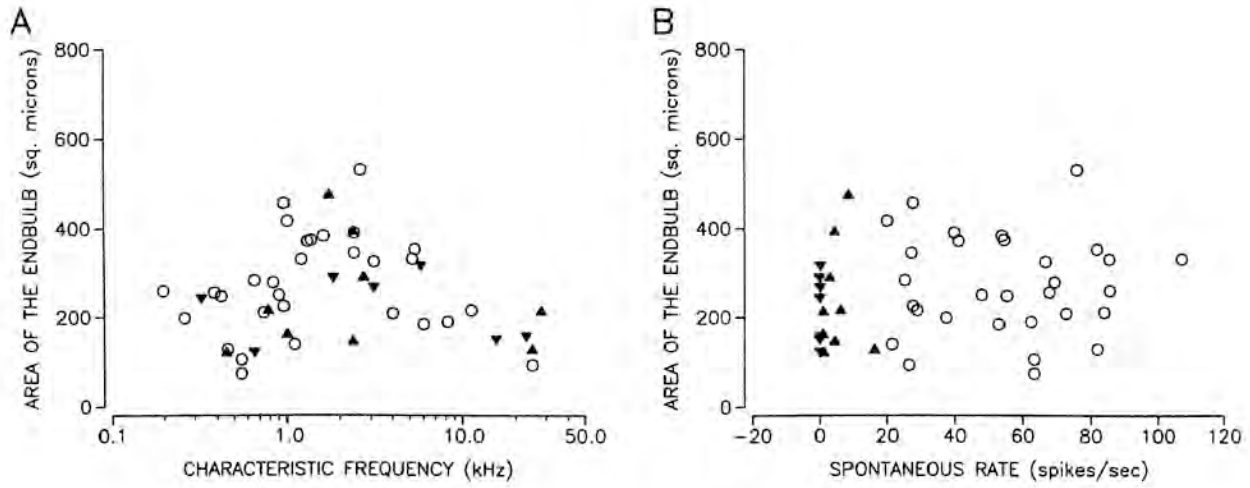

Figure 3. Scatter plots illustrating the distribution of endbulb size (silhouette area) with respect to fiber CF (A) and fiber SR (B). The largest endbulbs arise from fibers having CFs between 1-4 kHz; endbulb size does not appear correlated to fiber SR. Symbols: (O) SR > 18 s/s); (▲) SR 0.5-18 s/s; (▼) SR ≤ 0.5 s/s). (From Sento and Ryugo, 1989).

Table 1. Physiological and Morphological Data for Endbulbs Shown in Figure 2[1]

	a					b				
	CF (kHz)	*SR (s/s)*	*Endbulb Area (μm^2)*	*Form Factor*	*Soma Area (μm^2)*	*CF (kHz)*	*SR (s/s)*	*Endbulb Area (μm^2)*	*Form Factor*	*Soma Area (μm^2)*
A	8.2	62.7	189.1	0.543	427.0	23.0	0.4	157.3	0.354	395.9
B	2.4	27.3	344.6	0.584	717.1	1.7	8.6	475.2	0.455	533.5
C	0.6	25.3	282.9	0.534	857.2	0.3	0.1	243.1	0.345	431.2

Notes: [1] Columns a and b and rows A-C correspond to those in Figure 2.

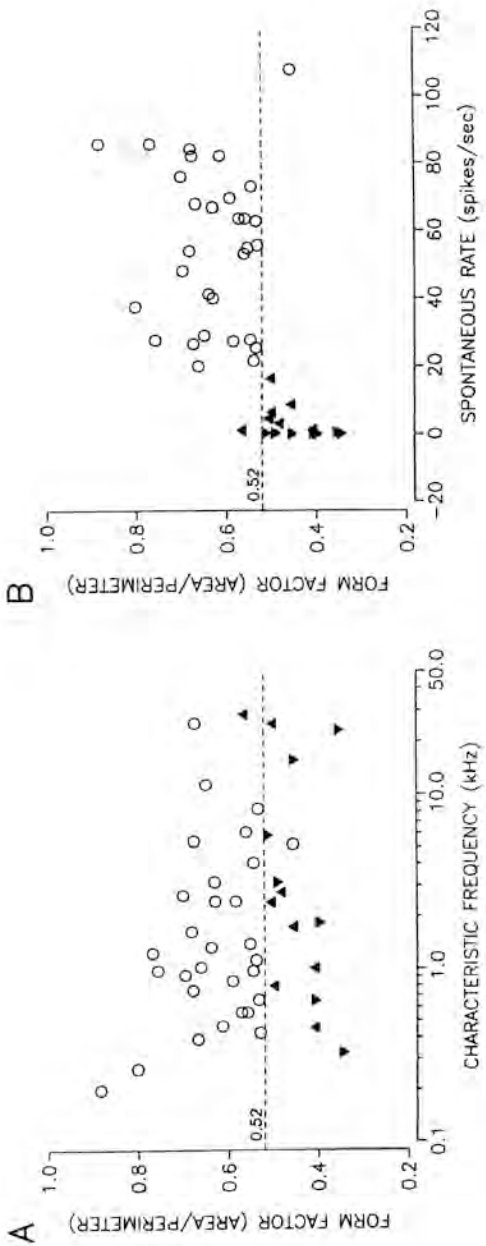

Figure 4. Scatter plots illustrating the distribution of form factor values (area divided by perimeter, units dropped) of the terminal endbulb with respect to fiber CF (A) and fiber SR (B). The value, 0.52, almost always separates endbulbs according to SR grouping, irrespective of fiber CF. Symbols as in Figure 3 (from Sento and Ryugo, 1989).

of low-medium SR fibers are of equal size compared to those of high SR fibers. Moreover, there is no difference in the areas of endbulbs between low SR fibers and medium SR fibers.

The Form Factor

The similarity in average size for endbulbs of high SR fibers versus low-medium SR fibers was unexpected, especially in light of their differences in appearance (Figs. 1, 2). We used the ratio, silhouette area divided by silhouette perimeter, to provide an objective value (called the form factor and having no units) for representing each endbulb (Table 1). This value tended into separate endbulbs into two populations according to SR, regardless of fiber CF or endbulb size (Fig. 4A). The form factor values for endbulbs of high SR fibers (range = 0.46-0.88; mean = 0.63 ± 0.02) were typically always larger than those for endbulbs of low-medium SR fibers (range = 0.34-0.56; mean = 0.45 ± 0.02). There was no systematic relationship between form factor and fiber CF.

Two endbulbs proved to be exceptions to the general rule using form factor values. Each endbulb arose from a different cat, yet other endbulbs in these cats followed the rule. It was of interest to note, however, that each exceptional endbulb originated from fibers having "extreme" physiological properties: One endbulb arose from a fiber having the highest SR in our population (107.5 s/s) and the other arose from a fiber having the highest CF (28.16 kHz). Nevertheless, we have demonstrated a method that identifies SR group of individual endbulbs, and reasoned that pairs of endbulbs which converged onto the same cell body could be assigned an SR group using form factor values.

3.2 Extracellularly Labeled Endbulbs: Convergent Pairs

Extracellular injections of HRP into the auditory nerve labeled large numbers of type I auditory nerve fibers. We found fewer than 100 instances where two endbulbs converged upon the same cell in the anterior division of the AVCN, and no instance where three endbulbs converged. The light microscopic data base consists of 19 darkly-stained and unambiguous cases where separate fibers gave rise to converging endbulbs and where both endbulbs were contained entirely within the tissue section. Endbulb pairs that were split across adjacent tissue sections were not analyzed.

The appearance of an endbulb pair is striking (Fig. 5). Typically, large caliber fibers (2-4 μm in diameter) approach the target bushy cell from different directions, often by abruptly reversing directions from their original trajectory. Auditory nerve fibers whose endbulbs are going to converge onto the same cell body do not necessarily travel side-by-side; that is, the ascending branches can be separated by more than 100 μm. The envelope fashioned by the terminal

Figure 5. Photomicrograph of a pair of endbulbs converging upon the same spherical bushy cell in the anterior part of the anteroventral cochlear nucleus. Their appearance and form factors (0.583 and 0.550) are typical for high SR endbulbs. Scale bar = 10 μm. (From Ryugo and Sento, 1991).

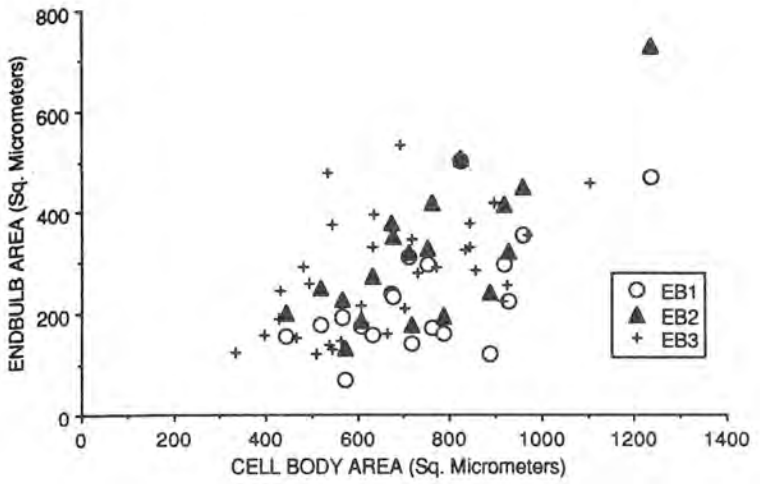

Figure 6. Scatter plot of endbulb silhouette area (ordinate) versus the area of its postsynaptic cell body (abcissa). These data are from endbulb pairs, with open circles representing the smaller endbulb (EB1) and solid triangles representing the larger (EB2) of the pair. Data from single fiber injections are indicated as EB3. On average, the larger the cell body, the larger the endbulbs that it receives. (From Ryugo and Sento, 1991).

swellings of each endbulb arbor establishes an irregular domain, and there appears to be a complementary interdigitation between domains of the separate endbulbs. Compared to the distinct appearance of endbulbs from fibers of different SR groups (e.g., Fig. 1), the endbulbs belonging to a pair have remarkably similar appearances (Fig. 5).

Endbulb Morphometry

Endbulb silhouette area (size) ranged from 69.6-726.5 μm^2. Pairs of terminal endbulbs contacting the same spherical bushy cell are usually different in size (Fig. 6). We call the smaller endbulb of the pair "endbulb 1" and the larger "endbulb 2". It also appears that the largest and the smallest endbulbs do not tend to form pairs. Instead, pairs of endbulbs tend to be correlated in size ($r = 0.864$, $p < 0.001$; Fig. 7). On average, the larger the cell body, the larger the endbulbs that it receives ($r = .584$, $p < 0.01$).

Form factor values for individual endbulbs of a pair ranged from 0.27-0.83. If endbulbs of fibers from the separate SR groups converged more-or-less randomly onto the same cell body, the ratio, form factor 1 (from endbulb 1)

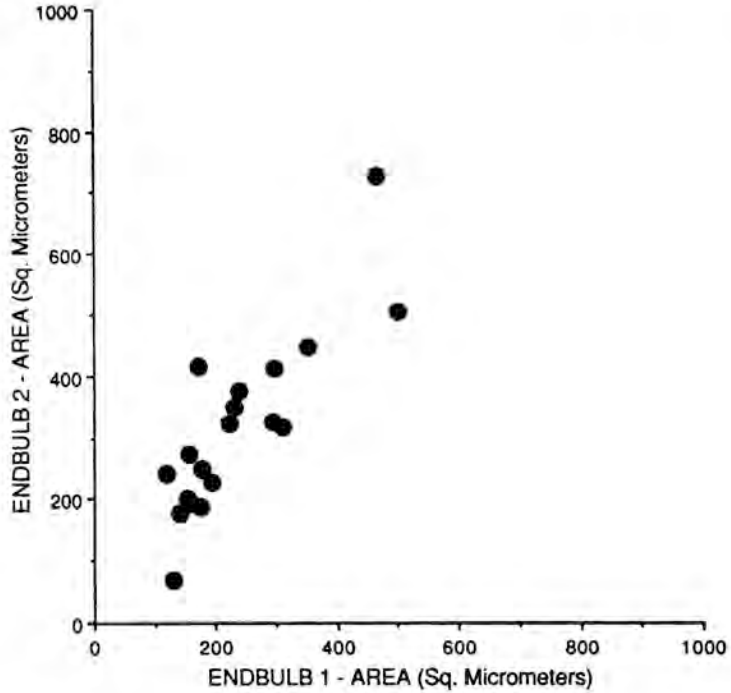

Figure 7. Scatter plot of silhouette area for endbulbs of a pair. The sizes of each endbulb are positively correlated with each other ($r = 0.864$, $p < 0.001$). These data emphasize the notion that within the range of endbulb size, endbulbs at opposite extremes do not form pairs. (From Ryugo and Sento, 1991).

divided by form factor 2 (from endbulb 2), could produce a range of values from 0.32-3.07. From a functional perspective, the convergence of endbulbs from fibers of different SR groups would produce a high SR spherical bushy cell due to the additive nature of the input activity; such mixing would certainly alter the SR distribution from nerve to nucleus. If, on the other hand, endbulbs of fibers from the same SR groups converged, this ratio should have a range of values near 1.0. In fact, the average ratio is 0.94 ± 0.03 with a range of 0.61-1.14. The implication from this observation is that only pairs of fibers belonging to the same SR group converge onto the soma of spherical bushy cells by way of their endbulbs.

The form factor value of endbulb 1 is correlated with that of endbulb 2 ($r = 0.707$, $p < 0.01$). These data also address the issue of whether or not fibers

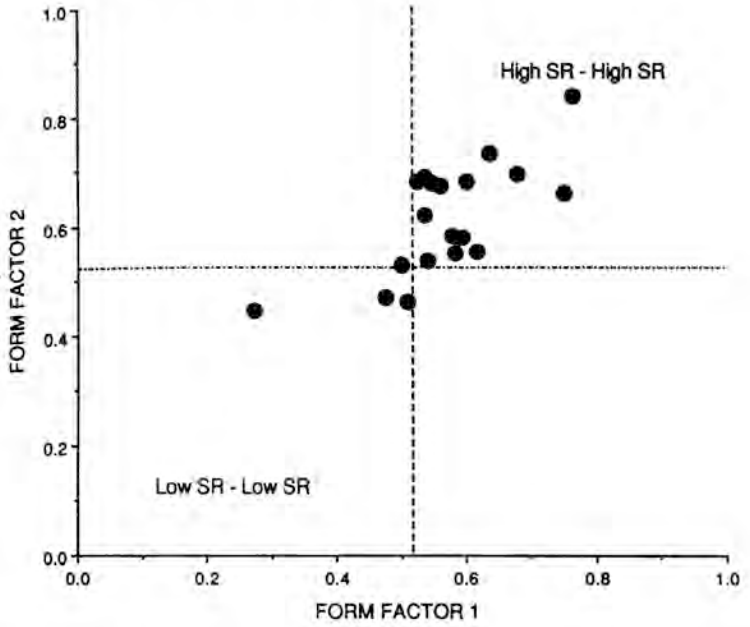

Figure 8. Scatter plot of the form factor value for the smaller endbulb (abcissa, endbulb 1) versus the form factor value for the larger endbulb (ordinate, endbulb 2) of a pair. Dashed lines are at 0.52, the cut-off between endbulbs of high and low SR fibers. The data suggest that fibers of both SR groups converge because of the presence of data points in the upper right and the lower left quadrants. The general lack of data points in the other quadrants suggest that endbulbs from fibers of different SR groups do not mix with one another. (From Ryugo and Sento, 1991).

of a particular SR group preferentially converge or do not converge upon the same spherical bushy cell (Fig. 8). For example, one mechanism for altering SR distribution in the AVCN would be if endbulbs of low SR fibers converge together but endbulbs of high SR fibers do not. If exclusively low SR fibers converge by way of endbulb pairs, then members of endbulb pairs would be expected to have form factor values less than 0.52 and data points should fall primarily into the lower left quadrant. On the other hand, if high SR fibers tend to form convergent endbulb pairs, then data points should lie primarily in the upper right quadrant. Lastly, if high and low SR fibers tend to form endbulb pairs, then data points should lie in the upper left and lower right quadrants. Our data, albeit limited, imply that convergence tends to occur

within but not across SR groups and that convergence is not an an exclusive feature of one SR group.

4. DISCUSSION

In the present study, we applied HRP labeling techniques combined with light and electron microscopy to study the synaptic relationship between endbulbs of Held and spherical bushy cells. Endbulbs have traditionally been described as the large axosomatic endings that arise from the population of thick auditory nerve fibers and terminate in the anteroventral cochlear nucleus (Held, 1896; Ramon and Cajal, 1909; Lorente de No, 1981). These thick fibers are myelinated (Arnesen and Osen, 1978; Cant and Morest, 1979); they arise from type I spiral ganglion neurons whose peripheral processes innervate one, or in rare instances two, inner hair cells (Kiang et al., 1982; Liberman and Oliver, 1984); and the endbulbs terminate exclusively on a distinct class of neurons called spherical bushy cells (Osen, 1969; Brawer and Morest, 1975; Cant and Morest, 1979; Ryugo and Fekete, 1982; Fekete et al., 1984; Sento and Ryugo, 1989). Because from 1-3 endbulbs contact a single neuron (Ramon y Cajal, 1909; Lorente de No, 1981), it seems that one inner hair cell must exert a rapid and powerful influence on a single spherical bushy cell. Our observations confirm and extend current knowledge of endbulb morphology and continue to build the foundation upon which to consider mechanisms of signal processing in the cochlear nucleus.

The endbulb of Held, containing numerous synaptic active zones and having an extensive apposition with the postsynaptic cell body, is presumed to faithfully transfer spike activity in the auditory nerve fiber to the postsynaptic spherical bushy cell. In addition, the endbulb is used to account for the presence of a small positive prepotential associated with units having primary-like discharge patterns (Pfeiffer, 1966; Bourk, 1976). The prepotential is thought to reflect a depolarization in the endbulb, followed 0.5 ms later by the discharge in the postsynaptic bushy cell (Molnar and Pfeiffer, 1968).

In this context, spherical bushy cells should preserve the signals from the nerve, and the population of primary-like units with prepotentials should reflect the physiological characteristics of the population of auditory nerve fibers. Although spherical bushy cells preserve the temporal patterns of spike discharges as evident in poststimulus time histograms (Rhode et al., 1983), they do not appear to preserve SR.

In the auditory nerve, approximately 40 percent of the fibers have SR $\leq$ 18 s/s and the rest have SR $>$18 s/s (Liberman, 1978; Evans and Palmer, 1980). In the AVCN, however, less than 15 percent of primary-like units with an unambiguous prepotential have SR $<$ 18 s/s (Molnar and Pfeiffer, 1968). These data are consistent with observations from Yin and his collaborators

(unpublished results) who are intracellularly recording and staining axons of the trapezoid body in cats. Of the primary-like units whose labeled axons project bilaterally to the medial superior olive and ipsilaterally to the lateral superior olive (indicative of spherical bushy cells; Cant and Casseday, 1986), roughly 12 percent of the units have SR $<$ 15 s/s. In short, the evidence suggests a transformation between auditory nerve and cochlear nucleus such that the average SR of primarlylike units with prepotentials (spherical bushy cells) is higher than that of auditory nerve fibers. Furthermore, prepotential units in the AVCN do not seem to exhibit the very low SR ($<$1 s/s) found in the auditory nerve.

Our studies explore possible anatomical substrates for this transformation of SR from nerve to nucleus. One way for SR distribution to change would be for endbulbs of fibers of different SR groups to converge upon the same spherical bushy cell. Direct evidence could be obtained by recording from and labeling a single auditory nerve fiber from each SR group whose endbulbs converged upon the same bushy cell. Given the improbability of such a feat however, we sought an indirect answer. We have previously demonstrated that the SR group of a particular auditory nerve fiber can be predicted on the basis of a morphometric algorithm for the terminal endbulb. That is, endbulb silhouette area divided by endbulb silhouette perimeter (units dropped) yields a "form factor" that separates endbulbs from the two SR groups (Sento and Ryugo, 1989). Our strategy was to apply this form factor analysis to convergent endbulb pairs but for which physiological features were unknown. Pairs of endbulbs having similar form factor values would imply convergence within SR groups; pairs having dissimilar form factor values would imply convergence across SR groups. Our results demonstrate that endbulb pairs converging onto the same cell body have very similar form factor values and imply that convergent endbulbs probably arise from fibers of the same SR group.

Incidentally, the relatively infrequent observations of HRP-labeled convergent endbulbs at the light microscopic level may reflect a sampling problem. Evidence from electron microscopy in population studies suggests that single HRP labeled endbulbs tend to have an unlabeled mate. That is, the HRP data produce a biased view of how many endbulbs actually converge. This situation may result if convergent axons do not tend to travel together as pairs. Our extracellular injections of HRP into the auditory nerve may simply fail to label both members of a pair. An alternative possibility is that convergent endbulbs arise from fibers innervating separate loci (and thus, separate frequency domains) of the cochlea. We reject this notion because the sharpness of tuning (Q_{10} value) of prepotential units is indistinguishable from that of auditory nerve units (Bourk, 1976); if fibers of different frequency characteristics converged, prepotential units would be expected to have broader frequency sensitivities.

SR proportions could also be transformed if high SR fibers gave rise to more endbulbs than did low SR fibers. This situation is not the case, however because individual auditory nerve fibers give rise to the same average number (mean $= 1.7 \pm 0.2$) of endbulbs (Ryugo and Rouiller, 1988). If endbulbs of low SR fibers converge but endbulbs of high SR fibers do not, SR distribution could also be altered. The presence of endbulb pairs exhibiting form factors indicative of both high and low SR fibers implies that restricted convergence does not occur. Perhaps the best explanation for the SR transformation in the cochlear nucleus is the observation that high SR endbulbs give rise to more axodendritic synapses than do low SR endbulbs (Ryugo et al., 1996). Spherical bushy cells emit several primary dendrites that radiate away from the cell body before each gives rise to its characteristic dendritic bush. The dendrites, however, do not "feed back" upon the parent cell body; rather, cell bodies of other spherical busy cells tend to nestle into the dendritic bush (e.g., Figures 3-12 and 3-15 of Lorente de Nó, 1981). Consequently, the postsynaptic dendrites are most likely not from the spherical bushy cell receiving the endbulb, but from a neighboring spherical bushy cell, and this structural substrate could serve to disperse preferentially the activity of high SR endbulbs (Ryugo and Sento, 1991). It remains to be determined whether collaterals arising from the endbulb (Brawer and Morest, 1975; Lorente de No, 1981; Ryugo and Fekete, 1982; Sento and Ryugo, 1989) might disperse activity sufficiently to alter the proportion of SR from nerve to nucleus.

ACKNOWLEDGMENTS

This work was supported by NIH grant RO1 DC00232. The authors wish to thank Tan Pongstaporn for his technical assistance, and Brad May, George A. Spirou, and Debora D. Wright for helpful discussions of the data.

REFERENCES

Arnesen, A.R. and Osen, K.K. (1978). The cochlear nerve in the cat: Topography, cochleotopy, and fiber spectrum. *J. Comp. Neurol., 178*, 661-678.

Bourk, T.R. (1976). *Electrical Responses of Neural Units in the Anteroventral Cochlear Nucleus of the Cat*. Ph.D. Dissertation, Massachusetts Institute of Technology, Cambridge, MA.

Brawer, J.R. and Morest, D.K. (1975). Relations between auditory nerve endings and cell types in the cat's anteroventral cochlear nucleus seen with the Golgi method and Nomarski optics. *J. Comp. Neurol., 160*, 491-506.

Cant, N.B. and Casseday, J.H. (1986). Projections from the Anteroventral Cochlear Nucleus to the Lateral and Medial Superior Olivary Nuclei. *J. Comp. Neurol, 247*, 457-476.

Cant, N.B. and Morest, D.K. (1979). Bushy cells in the anteroventral cochlear nucleus of the cat. A study with the electron microscope. *Neuroscience 4*, 1925-1945.

Cant, N.B. and Morest, D.K. (1984). The structural basis for stimulus coding in the cochlear nucleus of the cat. In: C.I. Berlin (Ed.), *Hearing Science, Recent Advances* (pp. 371-421). San Diego: College-Hill Press.

Evans, E.F. (1975). Cochlear nerve and cochlear nucleus. In: W.E. Keidel and W.D. Neff (eds.), *Handbook of Sensory Physiology*, (Vol. V, Part 2, pp. 1-108). Berlin: Springer-Verlag.

Evans, E.F. and Palmer, A.R. (1980). Relationship between the dynamic range of cochlear nerve fibers and their spontaneous activity. *Exp. Brain Res., 40*, 115-118.

Fekete, D.M., Rouiller, E.M., Liberman, M.C. and Ryugo, D.K. (1984). The central projections of intracellularly labeled auditory nerve fibers in cats. *J. Comp. Neurol., 229*, 432-450.

Held, H. (1893). Die centrale Gehorleitung. *Arch. Anat. Physiol. Anat. Abt.*, 201-248.

Ibata, Y. and Pappas, G.D. (1976). The fine structure of synapses in relation to the large spherical neurons in the anterior ventral cochlear (sic) of the cat. *J. Neurocytol., 5*, 395-406.

Kiang, N.Y.S., Rho, J.M., Northrup, C.C., Liberman, M.C., and Ryugo, D.K. (1982). Hair-cell innervation by spiral ganglion cells in adult cats. *Science, 217*, 175-177.

Kiang, N.Y.S., Watanabe, T., Thomas, E.C., and Clark, L.F. (1965). *Discharge Patterns of Single Fibers in the Cat's Auditory Nerve*. Cambridge, MA: MIT Press.

Koerber, K.C., Pfeiffer, R.R., Warr, W.B., and Kiang, N.Y.S. (1966). Spontaneous spike discharges from single units in the cochlear nucleus after destruction of the cochlea. *Exp. Neurol., 16*, 119-130.

Lenn, N.Y. and Reese, T.S. (1966). The fine structure of nerve endings in the nucleus of the trapezoid body and the ventral cochlear nucleus. *Am J. Anat., 118*, 375-389.

Liberman, M.C. (1978). Auditory-nerve response from cats raised in a low-noise chamber. *J. Acoust. Soc. Am., 63*, 442-455.

Liberman, M.C. (1982). Single-neuron labelling in the cat auditory nerve. *Science, 216*, 1239-1241.

Liberman, M.C. and Oliver, M.E. (1984). Morphometry of intracellularly labeled neurons of the auditory nerve: Correlations with functional properties. *J. Comp. Neurol., 223*, 163-176.

Lorente de No, R. (1981). *The Primary Acoustic Nuclei*. New York: Raven Press.

Molnar, C.E. and Pfeiffer, R.R. (1968). Interpretation of spontaneous spike discharge patterns of neurons in the cochlear nucleus. *Proceed. IEEE, 56*, 993-1004.

Osen, K.K. (1969). Cytoarchitecture of the cochlear nuclei in the cat. *J. Comp. Neurol., 136*, 453-484.

Pfeiffer, R.R. (1966). Anteroventral cochlear nucleus: Wave forms of extracellularly recorded spike potentials. *Science, 154*, 667-668.

Ramon, S. and Cajal (1909). *Histologie du Systeme Nerveux de l'Homme et des Vertebres*, (Vol. I, pp. 754-838). Madrid: Instituto Ramon y Cajal (1952 reprint).

Rhode, W.S., Oertel, D., and Smith, P.H. (1983). Physiological response properties of cells labeled intracellularly with horseradish peroxidase in cat ventral cochlear nucleus. *J. Comp. Neurol., 213*, 448-463.

Rouiller, E.M., Cronin-Schreiber, R., Fekete, D.M., and Ryugo, D.K. (1986). The central projections of intracellularly labeled auditory nerve fibers: An analysis of terminal morphology. *J. Comp. Neurol., 249*, 261-278.

Ryugo, D.K. and Fekete, D.M. (1982). Morphology of primary axosomatic endings in the anteroventral cochlear nucleus of the cat: A study of the endbulbs of Held. *J. Comp. Neurol. 210*, 239-257.

Ryugo, D.K. and Rouiller, E.M. (1988). The central projections of intracellularly labeled auditory nerve fibers in cats: Morphometric correlations with physiological properties. *J. Comp. Neurol., 271*, 130-142.

Ryugo, D.K. and Sento, S. (1991). Synaptic connections of the auditory nerve in cats: Relationship between endbulbs of Held and spherical bushy cells. *J. Comp. Neurol., 305*, 810-823.

Ryugo, D.K., Wu, M.M., and Pongstaporn, T. (1996). Activity-related features of synapse morphology: A study of endbulbs of Held. *J. Comp. Neurol., 365*, 141-158.

Sachs, M.B. and Abbas, P.J. (1974). Rate versus level functions for auditory-nerve fibers in cats: Tone-burst stimulation. *J. Acoust. Soc. Am. 56*, 1835-1847.

Sento, S. and Ryugo, D.K. (1989). Endbulbs of Held and spherical bushy cells in cats: Morphological correlates with physiological properties. *J. Comp. Neurol., 280,* 553-562.

Spoendlin, H. (1973). The innervation of the cochlear receptor. In: A.R. Møller (Ed.), *Mechanisms in Hearing* (pp. 185-229). New York: Academic Press.

Tsuchitani, C. (1978). Lower auditory brain stem structures of the cat. In: R.F. Naunton and C. Fernandex, (Eds.), *Evoked Electrical Activity in the Auditory Nervous System* (pp. 373-401). New York: Academic Press.

Walsh, B.T., Miller, J.B., Gacek, R.R., and Kiang, N.Y.S. (1972). Spontaneous activity in the eighth cranial nerve of the cat. *Int. J. Neurosci., 3,* 221-236.

Warr, W.B. (1982). Parallel ascending pathways from the cochlear nucleus: Neuroanatomical evidence of functional specialization. *Contrib. Sens. Physiol., 7,* 1-38.